Geomechanics and Engineering, *Vol. 6, No. 4 (2014) 359-376*
DOI: http://dx.doi.org/10.12989/gae.2014.6.4.359

A new thermal conductivity estimation model for weathered granite soils in Korea

Gyu-Hyun Go [1], Seung-Rae Lee [*1], Young-Sang Kim [2], Hyun-Ku Park [3] and Seok Yoon [1]

[1] *Department of Civil Engineering, Korean Advanced Institute for Science and Technology*, 291 *Daehak-ro, Yuseong-gu, Daejeon* 305-701, *Republic of Korea*
[2] *Department of Marine and Civil Engineering, Chonnam National University*, 50 *Daehak-ro, Yeosu, Jeonnam* 550-749, *Republic of Korea*
[3] *Engineering & Construction Group Civil Engineering Division, Samsung C&T*, 1321-20 *Seocho 2-Dong, Seocho-Gu, Seoul* 137-857, *Republic of Korea*

(*Received June* 20, 2013, *Revised October* 31, 2013, *Accepted November* 19, 2013)

Abstract. Thermal conductivity of ground has a great influence on the performance of Ground Heat Exchangers (GHEs). In general, the ground thermal conductivity significantly depends on the density (or porosity) and the moisture content since they are decisive factors that determine the interface area between soil particles which is available for heat transfer. In this study, a large number of thermal conductivity experiments were conducted for soils of varying porosity and moisture content, and a database of thermal properties for the weathered granite soils was set up. Based on the database, a 3D Curved Surface Model and an Artificial Neural Network Model (ANNM) were proposed for estimating the thermal conductivity. The new models were validated by comparing predictions by the models with new thermal conductivity data, which had not been used in developing the models. As for the 3D CSM, the normalized average values of training and test data were 1.079 and 1.061 with variations of 0.158 and 0.148, respectively. The predictions became somewhat unreliable in a low range of thermal conductivity values in considering the distribution pattern. As for the ANNM, the 'Logsig-Tansig' transfer function combination with nine neurons gave the most accurate estimates. The normalized average values of training data and test data were 1.006 and 0.954 with variations of 0.026 and 0.098, respectively. It can be concluded that the ANNM gives much better results than the 3D CSM.

Keywords: thermal conductivity; predictive model; artificial neural network model; transfer function; weathered granite soils

1. Introduction

In general, ground-surface temperatures fluctuate with seasonal air temperature, while the temperature below a depth of 15 m remains relatively constant throughout the year because the overlying ground acts as an insulator (Bennett 2008, Olgun *et al*. 2012). Ground-Source Heat Pump (GSHP) systems utilize this relatively constant temperature as an energy source by circulating fluid through heat exchangers. Owing to this tremendous and free source of stored

*Corresponding author, Professor, E-mail: srlee@kaist.ac.kr

http://www.techno-press.org/?journal=gae&subpage=7 ISSN: 2005-307X (Print), 2092-6219 (Online)

energy, the GSHP systems can guarantee high heat efficiency compared to other heating and cooling systems. In order to exploit this ground energy, a heat exchanger is installed in the GSHP system and buried in various ways. Though there are others, traditionally, vertical closed-loop heat exchangers are commonly used and they need high drilling costs at the initial stage of construction. Recently, however, to reduce high construction costs, these heat exchangers can be installed inside foundation piles of building, and the piles are called energy piles (Pahud *et al*. 1999, Laloui *et al*. 2003, Brandle 2006). Then they play a role not only as a structural support but also as a carrier for heat exchange. Because the heat exchangers are just installed inside existing piles without any additional drilling, the depth is limited to the length of piles (about 20 m). Therefore, energy pile heat exchange occurs usually in a shallow depth, and the design of energy piles should accommodate the thermal properties of soil existing in the relatively shallow depths.

In the design of energy piles, the most important factor is the thermal conductivity of ground in which the heat exchangers are installed. Therefore a reasonable estimation of those thermal properties facilitates an efficient design of GSHP systems by providing more accurate estimates of heat transfer between the ground loop heat exchanger and the surrounding soil (Hart and Whiddon 1984). Unfortunately, there are not enough thermal property databases that reflect the characteristics of Korean weathered-granite soils. Moreover, it is uncertain whether current estimation models are applicable to Korean weathered granite soils. For these reasons, this study focused on Korean weathered-granite soils, and developed a database of relevant thermal properties. Based on this new database, a 3D CSM and an ANNM were proposed for accurate estimation of thermal conductivity. Finally, the new models were validated by comparing model predictions with new thermal conductivity data that are not used in developing the models.

2. Thermal conductivity test

There are two methods for measuring the thermal conductivity: the steady state method and the non-steady state method. The steady state method measures the heat velocity needed to keep the temperature constant between two different materials. The representative equipment used for the steady state method is a Heat Flow Meter shown in Fig. 1(a) (Netzsch 2013). Though the test procedure is simple, it takes long time to accomplish, and if the surface materials are unstable, this test may give results of low accuracy. On the other hand, the non-steady state method is based on a linear heat source theory. The material properties are determined while the sample temperature is still changing. The main advantage of the non-steady state technique is its short measurement time. The TP08 Probe (Hukseflux 2006) is a typical equipment used for the non-steady state method. It only takes 200 s to obtain the results.

In order to compare the results from these methods, thermal conductivity tests were carried out using the two identical soil samples. Fig. 2 illustrates the variation of thermal conductivity with the dry density, as determined by the two different methods. In most cases, both methods predicted similar values of thermal conductivity at the same dry density (See the vertical bar in Fig. 2), even though there was a slight difference in the two predictions for sand. Thus, the results are quite similar, regardless of which test methodology is used.

This study selected the TP08 probe as a measurement tool because it has great advantages in developing the database due to its short measurement time. The TP08 probe is composed of parts shown in Fig. 1(b): ① wire, ② base, ③ needle, ④ temperature sensor, ⑤ heating wire, and ⑥ thermocouple junction. As shown in Fig. 1(b), once heat is injected by the needle probe, it induces

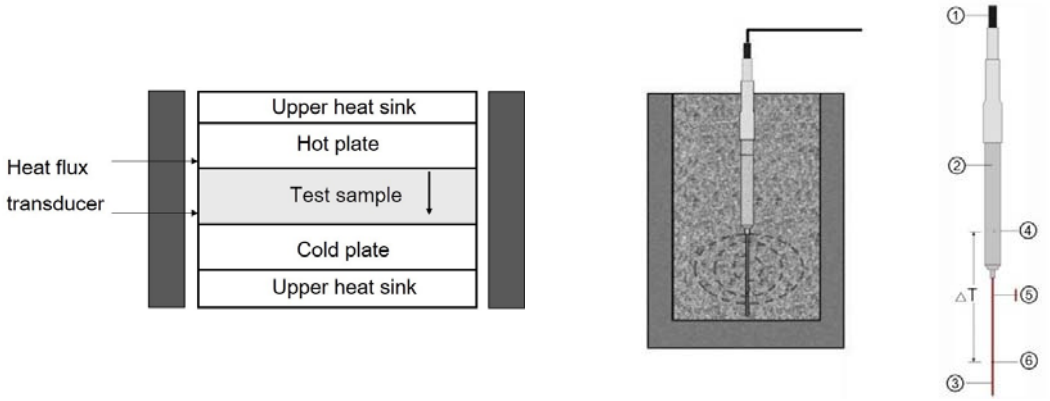

Fig. 1 Thermal conductivity measurement equipment: (a) Schematic design of HFM equipment; (b) Schematic layout of TP08 Probe (Hukseflux 2006)

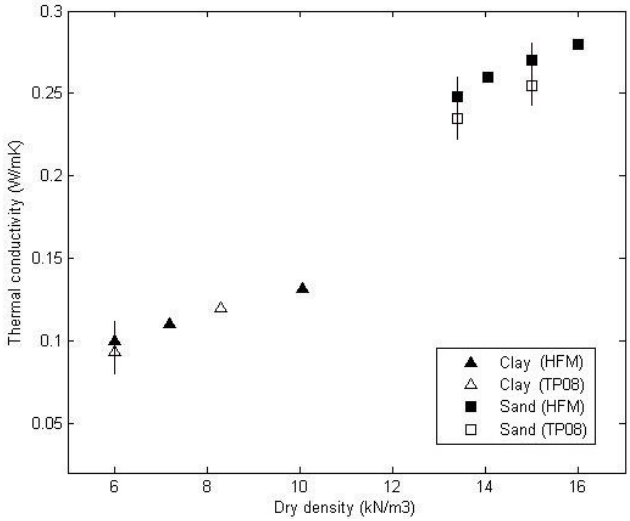

Fig. 2 Comparison of results from TP08 and HFM in dry state

a thermo-electromotive force, after which the thermal conductivity can be measured in a non-steady state.

3. Development of database

3.1 Test materials

The weathered granite soils from Gangwon Inje (W1), Gangwon Pyungchang (W2), Gangwon Taebaek (W3), Busan Geumjung (W4), Sejong Yeongi (W5) and Joomoonjin sand (Sand) in

Korea were sampled and used in the thermal conductivity tests. Table 1 summarizes the basic properties of these samples. Because the porosity of an undisturbed sample was in the range of 0.4 ~ 0.5, the disturbed soil for the thermal conductivity test was made in this range. Joomoonjin sand is poorly graded, but the weathered granite soils are quite similar to other well graded soils. Also, as shown in Fig. 3, the weathered granite soils can be regarded as non-plastic soils due to the low proportion of fine particles in those soils.

A quantitative mineral analysis of the weathered granite soils was performed by X-ray diffraction (XRD – Table 2, Fig. 4). The thermal conductivity of the soil particles (λ_{sp}) was obtained from the literature (Horai 1971) and a geometric-mean-based model (Eq. (1)). The geometric-mean-based model is a kind of theoretical model based on an arithmetic mean, geometric mean and harmonic mean.

$$\lambda_s = \prod_j \lambda_{m_j}^{x_j}, \quad \text{with} \sum_j x_j = 1 \tag{1}$$

where λ_{m_j} is the thermal conductivity of j^{th} mineral, and x_j is a composition ratio of j^{th} mineral.

Table 1 Basic properties of soil samples

Soil	Porosity*	Coefficient of uniformity C_u	Coefficient of curvature C_c	Specific gravity G_s	USCS*
Sand	0.45	2.06	1.05	2.65	SP
W1	0.47	6.22	0.96	2.59	SP
W2	0.46	4.89	1.51	2.66	SW
W3	0.45	11.67	1.08	2.55	SW
W4	0.53	8.53	1.58	2.54	SW
W5	0.44	6.55	0.97	2.58	SP

*Porosity (undisturbed); USCS: Unified Soil Classification System

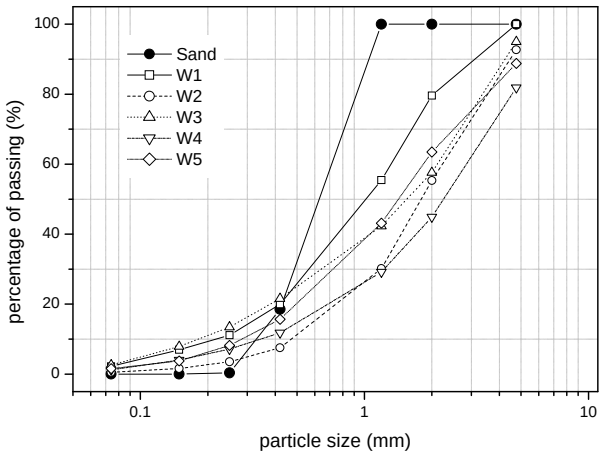

Fig. 3 Particle size distribution of samples

Table 2 Results of mineral quantitative analysis (XRD)

Soil	Mineral portion (%)*								
	Quartz (7.69)	Microcline (2.49)	Albeit (1.96)	Kaolin $(3.0)^+$	Orthoclase (2.32)	Muscovite (3.48)	Illite $(3.0)^+$	Chlorite (5.15)	λ_{sp} (W/m·K)
Sand	92.0	5.0	–	–	3.0	–	–	–	7.01
W1	38.3	17.0	12.9	13.9	–	12.2	7.5	1.1	4.22
W2	28.6	19.0	28.5	9.0	–	6.8	-	1.1	3.49
W3	32.9	19.3	5.0	26.2	–	4.9	5.5	3.0	4.04
W4	38.5	–	23.5	17.9	19.2	–	–	0.6	3.88
W5	28.2	21.8	24.6	13.8	–	5.9	4.2	0.8	3.50

*Provided by KIGAM, $^+$Assumed referring to a literature (Johansen 1975)

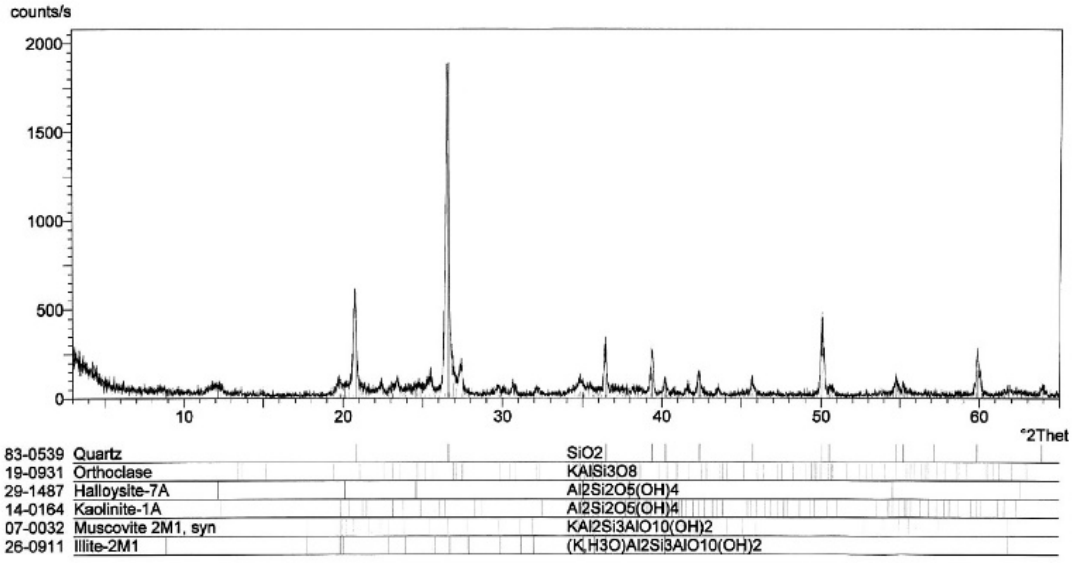

Fig. 4 Results of mineral quantitative analysis

As for the Joomoonjin sand, the proportion of quartz appeared to be more than 90% of total mineral composition. This means that there are great differences in the mineral compositions of weathered granite soils and joomoonjin sand. The implication is that it may be difficult to apply current models to weathered granite soils in Korea because a number of current prediction models are applicable to pure sand or gravel which has different mineral compositions compared to the weathered granite soils (Farouki 1986, Park 2011).

3.2 Test results

It is widely known that the moisture content greatly influences the thermal conductivity of soils (Kersten 1949, Penner *et al*. 1975, Salomone and Kovacs 1984, Park 2011). The moisture content

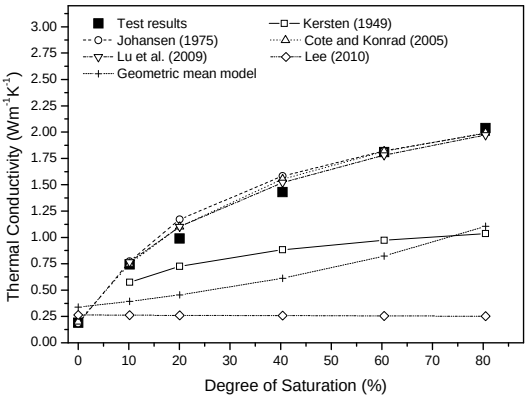

(a) Joomoonjin sand (porosity = 0.48)

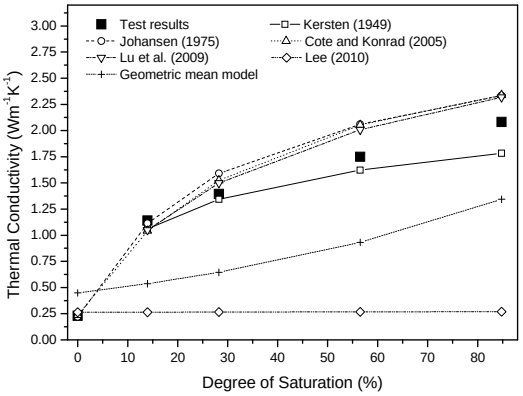

(b) Joomoonjin sand (porosity = 0.42)

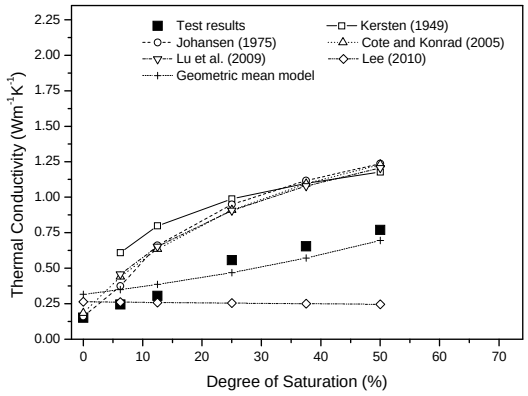

(c) W1-1 (porosity = 0.51)

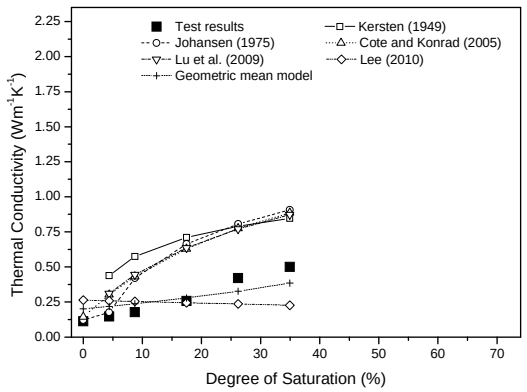

(d) W1-2 (porosity = 0.59)

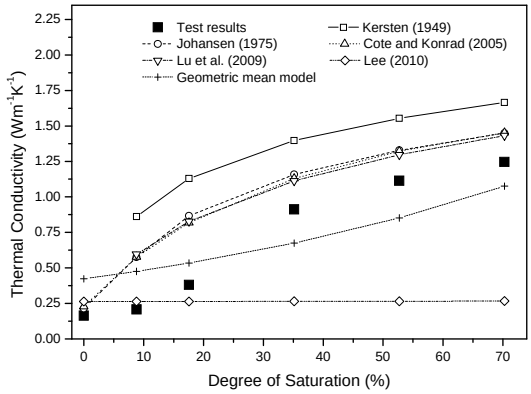

(e) W2-1 (porosity = 0.43)

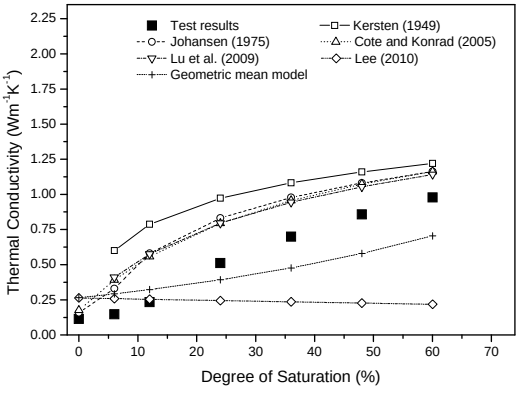

(f) W2-2 (porosity = 0.53)

Fig. 5 Comparison results of experiments and previous prediction models (Park *et al*. 2012)

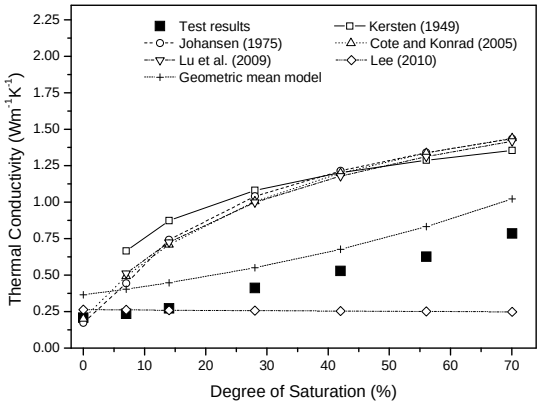

(g) W3-1 (porosity = 0.48)

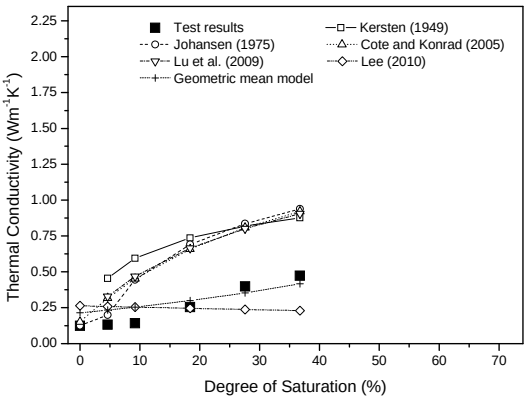

(h) W3-2 (porosity = 0.58)

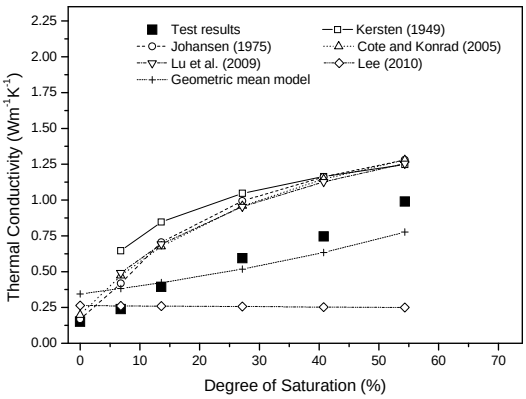

(i) W4-1 (porosity = 0.48)

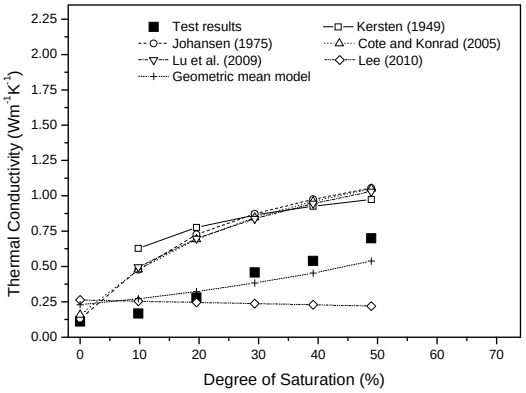

(j) W4-2 (porosity = 0.56)

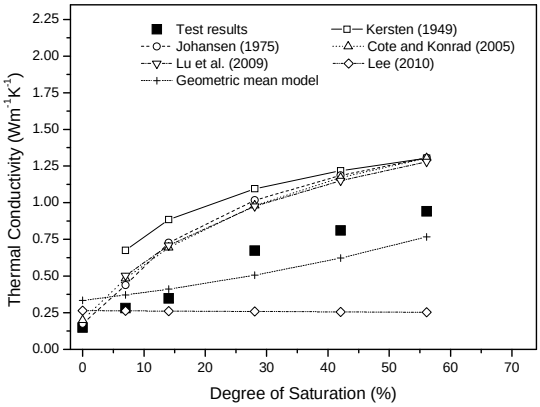

(k) W5-1 (porosity = 0.48)

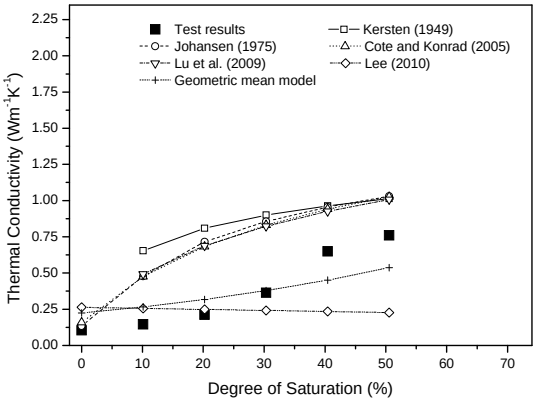

(l) W5-2 (porosity = 0.56)

Fig. 5 Continued

Table 3 Previous prediction models applied to thermal conductivity test analysis

Model	Prediction formula*	Remark
Kersten (1949)	$\lambda = 0.1442\ (0.7 \log w + 0.4) \cdot 10^{0.6243\rho_d}$	ρ_d in g/cm^3
Johansen (1975)	$\lambda = (\lambda_{sat} - \lambda_{dry}) \cdot (0.7 \log S_r + 1.0)$, where $\lambda_{sat} = \lambda_{sp}^{1-n}\lambda_w^{n}$, $\lambda_{dry} = (0.137\rho_d + 64.7) / (2700 - 0.947\rho_d) \pm 20\%$	ρ_d in kg/m^3
Côté and Konrad (2005)	$\lambda = (\lambda_{sat} - \lambda_{dry}) \cdot [kS_r / (1 + (k-1)S_r)] + \lambda_{dry}$ where k = empirical parameter, $\lambda_{dry} = \chi 10^{-\eta n}$ $\chi = 0.75$ for soil, η = particle shape parameter, n = porosity	Coarse-fine grained soil
Lu *et al*. (2007)	$\lambda = (\lambda_{sat} - \lambda_{dry}) \cdot (\exp\{\alpha[1 - S_r^{\alpha-1.33}\}$, where $\alpha = 0.96$ for coarse soil, $\lambda_{dry} = -0.56n + 0.51$, n = porosity	Coarse grained soil
Lee (2010)	$\lambda = (0.42\ \rho_d - 0.62) \cdot w + 0.2633$	Weathered granite soil
Geometric mean model	$\lambda = \Pi\ \lambda_{mj}^{x_j}$, x = volume fraction, j = soil grain, pore water, and pore air	Theoretical model

*w: moisture content, S_r: degree of saturation, λ_{sp}: thermal conductivity of soil particle, λ_w: thermal conductivity of water (= 0.57 Wm^{-1}K^{-1})

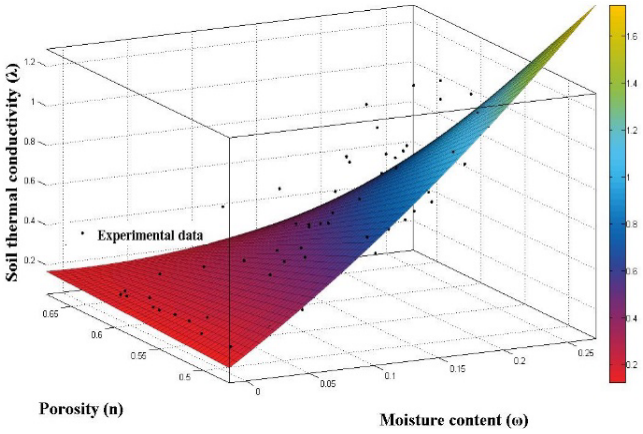

Fig. 6 3-D curved surface model based on experimental data

3.3 Estimation model based on database

Here a new thermal conductivity estimation model was proposed considering the effects of porosity and moisture content. Based on the newly established database, a 3-D Curved Surface Model (CSM) (Fig. 6) was developed, and its equation (Eq. (2)) is represented as a function of

porosity and moisture content. It was taken by the polynomial regression analysis from the surface fitting tool box in MATLAB Program, and this tool box can determine the optimum equation which yields the highest coefficient of determination values. The range of conditions is limited to the following: 0 ~ 25% moisture content and 0.25 ~ 0.65 porosity. This model was based on the experimental database for weathered granite soils, and thus it can accurately predict the results for weathered granite soils.

$$f(\omega, n) = 0.66 + 20.57 \cdot \omega - 0.94 \cdot n - 3.51 \cdot \omega^2 - 28.6 \cdot \omega \cdot n \tag{2}$$

where ω is the moisture content, and n is the porosity.

4. Thermal conductivity artificial neural network model

The Artificial Neural Network Model (ANNM) is a mathematical model which imitates the network system of a human brain. This model has been widely used in various geotechnical engineering areas, including the estimation of consolidation settlement and undrained shear strength of soils (Lee *et al*. 2000, Min *et al*. 2000, Kim 2005). In this study, an ANNM was developed based on thermal conductivity data, for estimating the thermal properties of weathered granite soils in Korea.

As shown in Fig. 7, the ANNM consists of a multilayer neural network which includes Input layer (I) – Hidden layer (H) – Output layer (O). In each layer, there are several neurons replicating a standard unit of human nervous tissue and they are connected with neurons in other layers by specific weights and biases. The input data of neurons in each layer are multiplied by weights, and then the sum of these values are handled by a transfer function. The resulting values are then transferred to the next layer as input data. The building process of an ANNM can be divided into two steps. The first step is a training phase, in which the weights of neurons in each layer are adjusted. In this step, the ANNM is able to learn about the optimum weights that can generalize the given data by itself. Next step is a testing phase where the developed model is verified by comparing the prediction data with new experimental data. The data should not be used in developing the model.

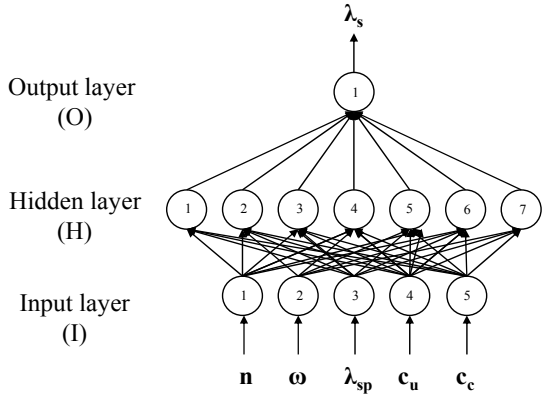

Fig. 7 Artificial neural network model for estimating thermal conductivity

Table 4 Characteristics of input data used in neural network training and testing

	1	2	3	4	5
Soil	Porosity	Moisture content, ω (%)	λ_{sp}* (W/m•K)	Coefficient of uniformity C_u	Coefficient of curvature C_c
W1	0.47	0 ~ 22	4.22	6.22	0.96
W2	0.46	0 ~ 22	3.49	4.89	1.51
W3	0.45	0 ~ 23	4.04	11.67	1.08
W4	0.53	0 ~ 25	3.88	8.53	1.58
W5	0.44	0 ~ 20	3.50	6.55	0.97

* Soil particle's thermal conductivity estimated by geometric mean model

4.1 Database of weathered granite soils

As specified in Section 3, in this study a thermal conductivity database was set up for weathered granite soils sampled in Gangwon Inje (W1), Gangwon Pyungchang (W2), Gangwon Taebaek (W3), Busan Geumjung (W4), and Sejong Yeongi (W5). Five fundamental soil properties were selected as input variables for the model (Table 4), and about 100 data points were used for the ANNM. Seventy-four of these data points were used as 'training data' to develop the ANNM, and 30 points of randomly selected data were used as 'testing data' to verify the applicability of the ANNM. The input data were normalized to a value of range within [0, 1] to perform the training job more efficiently.

4.2 Optimization technique

In general, an 'error back-propagation algorithm' is used for training multilayer neural networks because it is useful for developing non-linear relationships between input and output data. The 'Levenberge-Marquardt technique' (provided in the Matlab Toolbox) was used for optimizing the weights and biases. This technique improves the training efficiency of the error back-propagation algorithm (Demuth and Beale 1992). The training phase was stopped when it reached a maximum Epoch, or when the mean squared error (mse) defined by Eq. (3) converged below the mean-squared-error goal (0.005).

$$mse = \frac{1}{n}\sum_{k=1}^{n}\left(a(k) - t(k)\right)^2 \tag{3}$$

where $a(k)$ is the thermal conductivity predicted by the ANNM, $t(k)$ is the measurement data of thermal conductivity, and n is the total number of data.

4.3 Decision of optimization model

In order to build up the ANNM, the five fundamental input parameters shown in Table 4 were selected. Since the accuracy of the model depends on the number of neurons in the hidden layer and type of transfer function, different combinations of transfer function (Log-sigmoid, Tan-

Table 5 Combination of transfer functions and R^2 values of each model

Transfer function	Number of neurons	R^2 of training data	R^2 of testing data
Logsig - Linear	7	0.90	0.80
Logsig - Logsig	8	0.87	0.85
Logsig - Tansig	9	0.93	0.84
Tansig - Linear	10	0.89	0.83
Tansig - Logsig	7	0.85	0.87
Tansig - Tansig	6	0.85	0.82

sigmoid, or Linear) were applied to the model (Table 5). Then the analysis was performed to obtain the coefficient of determination (R^2) for the training and testing data by increasing the number of neurons from 1 to 10. Finally, the most accurate model was selected as the optimized estimation model.

Figs. 8(a), (c), (e), (g), (i) and (k) show the variation of coefficient of determination (R^2) for the training and testing data according to the number of neurons in the hidden layer. The coefficient of determination of the training data was prone to increase as the number of neurons increased, while the coefficient of determination of the testing data fluctuated, rather than to increase consistently. The increase in R^2 in the training data is resulted from the 'remember effect' during the training phase rather than 'learning performance improvement' due to the increase in neurons. Figs. 8 (b), (d), (f), (h), (j) and (l) show the comparison results between predictions and experiments for the training and testing data, and their R^2 values are enumerated in detail.

Though all six models showed high accuracy in the prediction (> 0.8 of R^2), the model using the Logsig–Tansig transfer function combination was selected as the best. As shown in Fig. 8(e), as the number of neuron increases, the coefficient of determination (R^2) also shows a tendency

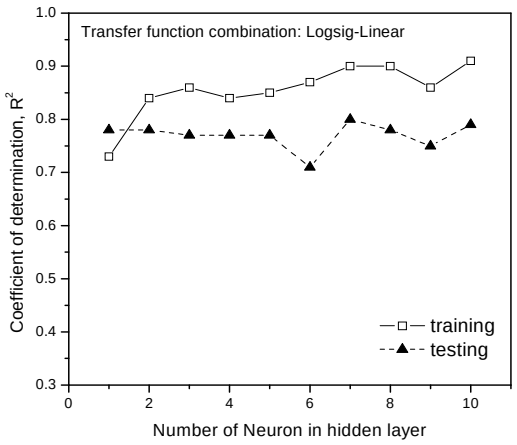

(a) R^2 variation with number of neurons in hidden layer

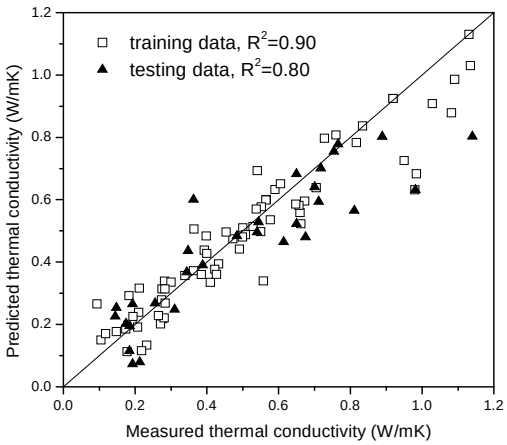

(b) Logsig - Linear model with 7 neurons

Fig. 8 Comparison of R^2 values for different models

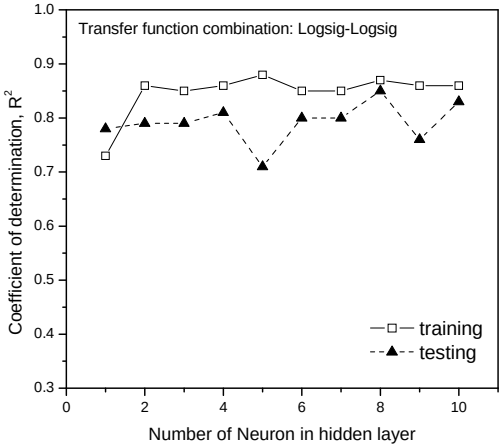

(c) R^2 variation with number of neurons in hidden layer

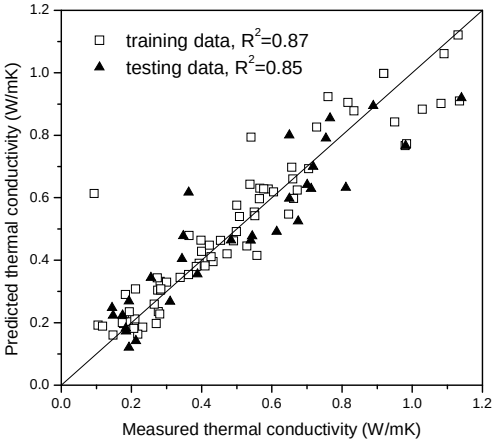

(d) Logsig - Logsig model with 8 neurons

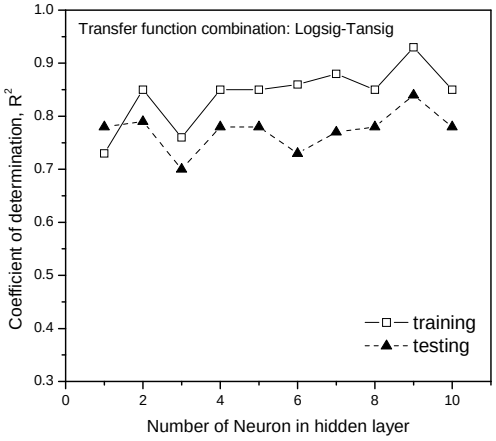

(e) R^2 variation with number of neurons in hidden layer

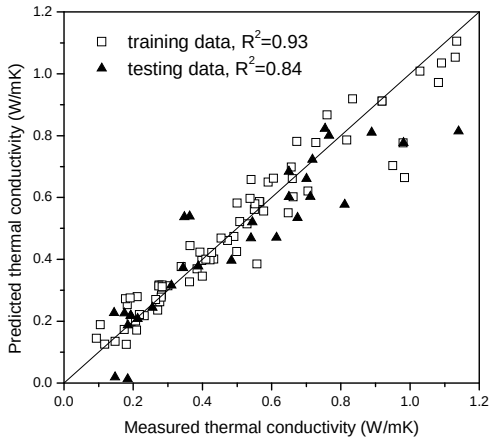

(f) Logsig - Tansig model with 9 neurons

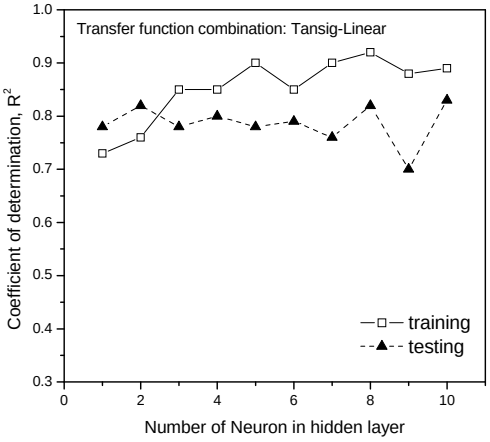

(g) R^2 variation with number of neurons in hidden layer

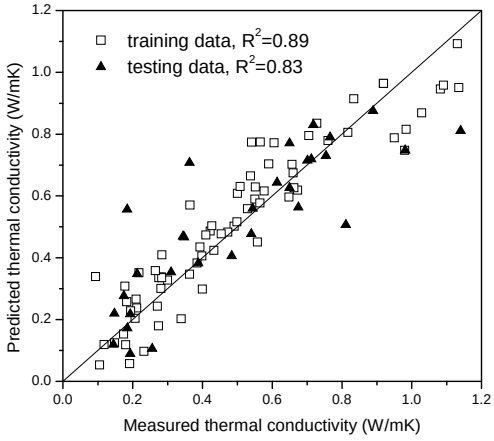

(h) Tansig - Linear model with 10 neurons

Fig. 8 Continued

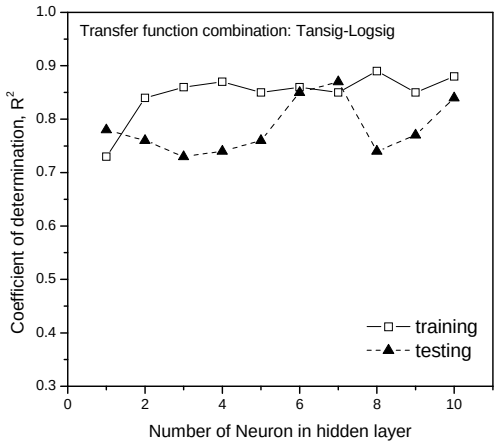

(i) R^2 variation with number of neurons in hidden layer

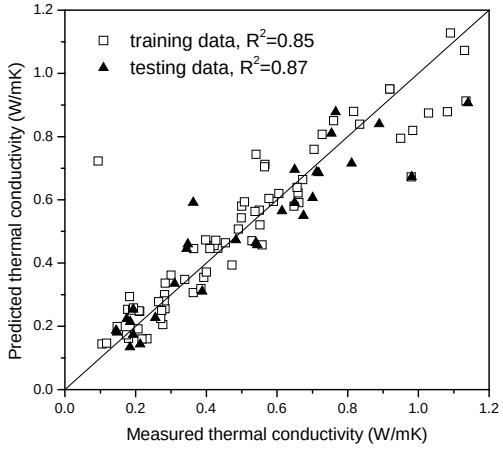

(j) Tansig - Logsig model with 7 neurons

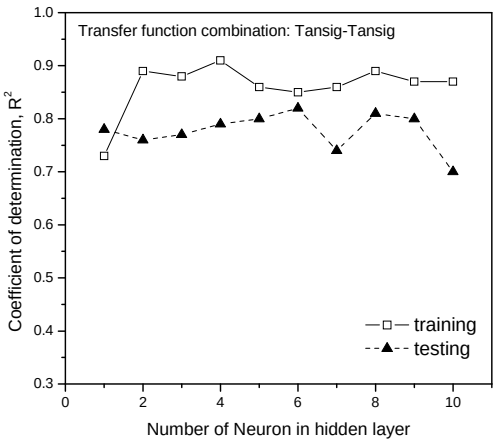

(k) R^2 variation with number of neurons in hidden layer

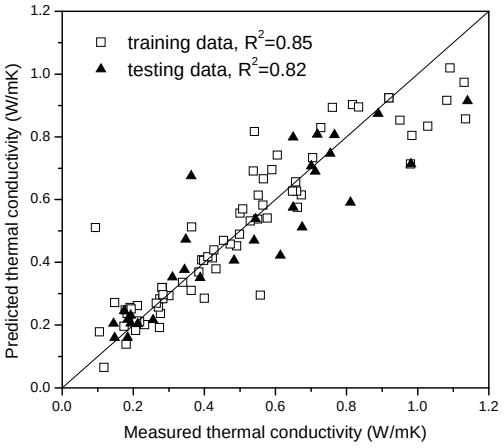

(l) Tansig - Tansig model with 6 neurons

Fig. 8 Continued

to increase in both training and testing data. Therefore, the model (Logsig–Tansig) with 8 neurons yields the highest accuracy among others; it represents the R^2 value of 0.93 and 0.84, respectively.

5. Results

This study verified the predictive accuracy of the developed models by comparing the results obtained by the ANNM, 3D CSM (Eq. (2)) and the previous estimation models (Table 3). Fig. 9 plots the prediction results of each model using the training and testing data. For the reasonable verification, new thermal conductivity data which had not been used in developing the model were used for testing. As shown in Fig. 9, both the ANNM and 3D CSM provide good predictive accuracy compared to the previous estimation models for both training and test data. The empirical

models (e.g., Kersten (1949), Johansen (1975), Côté and Konrad (2005), and Lu *et al*. (2007)) have a tendency to overestimate the measured values, while the theoretical (geometric mean) model underestimates them. Though the Lee model (2010) is also an empirical model, it is not adaptable for the samples considered in this study because the model was developed primarily for the heavily compacted weathered granite soil of which the dry unit weight was larger than 15 kN/m^3.

Based on the results of Table 6, the ANNM and 3D CSM seem to be better than the others for the prediction, and hence their predictive accuracy is compared in more details. Figs. 10 and 11 show the comparison of normalized values for the two models. As for the 3D CSM, the normalized average values of training and test data were 1.079 and 1.061, respectively, with variations of 0.158 and 0.148. The predictions became unreliable for low range thermal conductivity

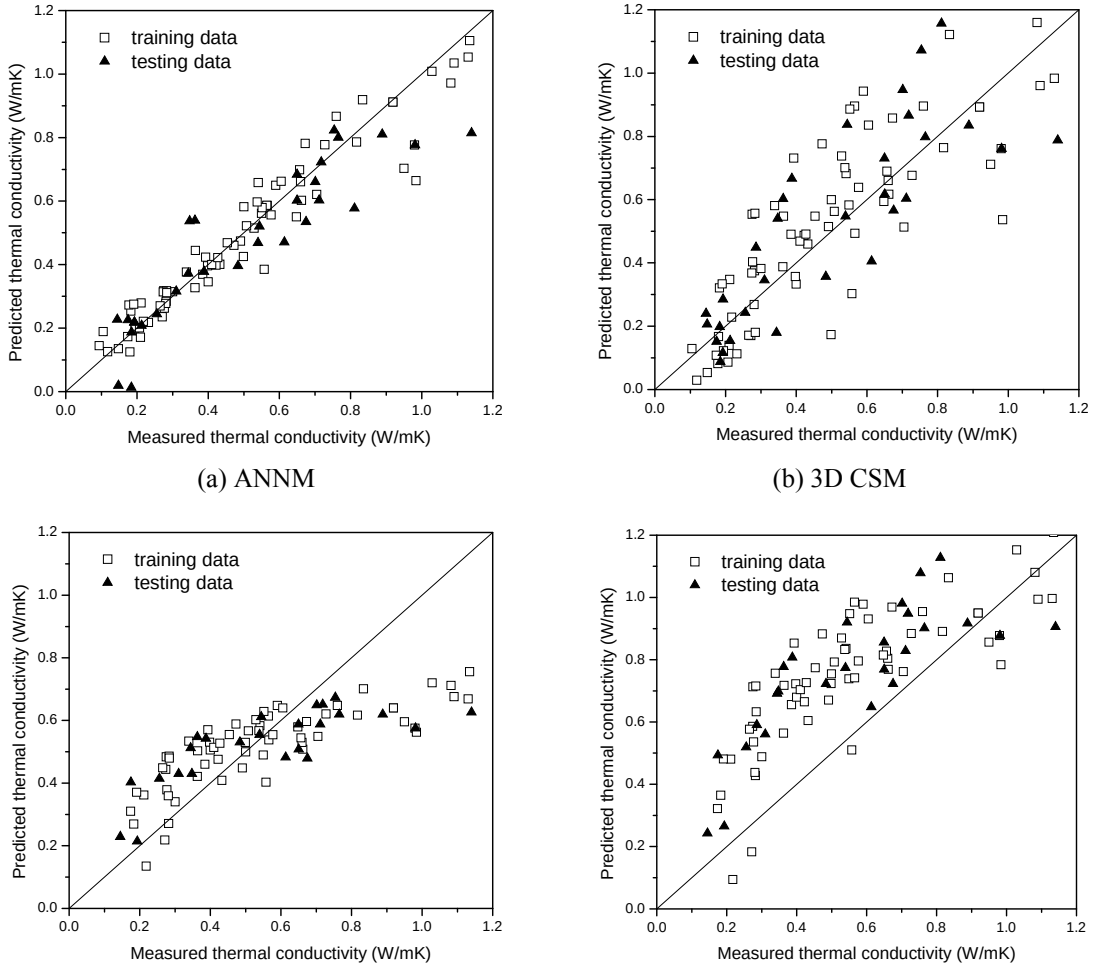

(a) ANNM (b) 3D CSM

(c) Kersten (1949) model (d) Johansen (1975) model

Fig. 9 Comparison results of each model

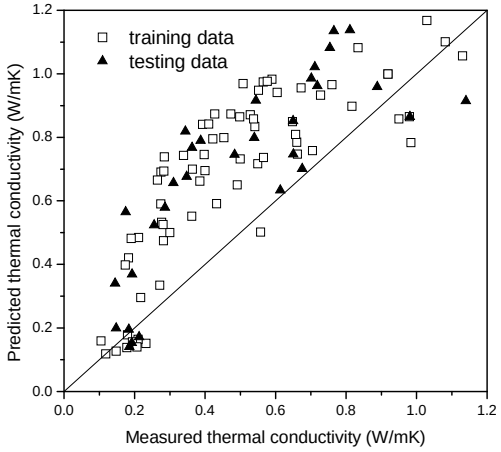

(e) Côté and Konrad (2005) model

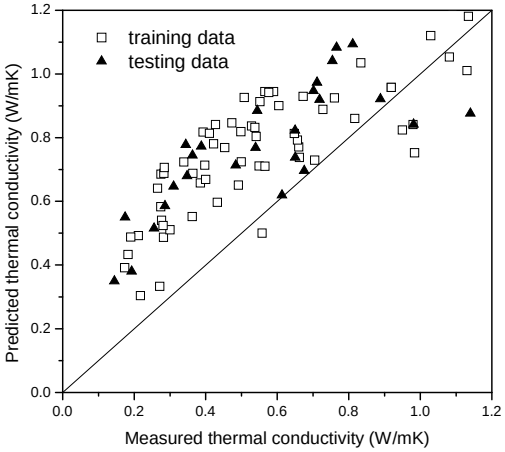

(f) Lu *et al*. (2007) model

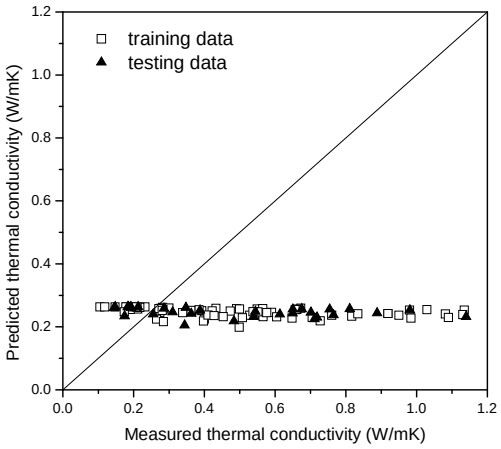

(g) Lee (2010) model

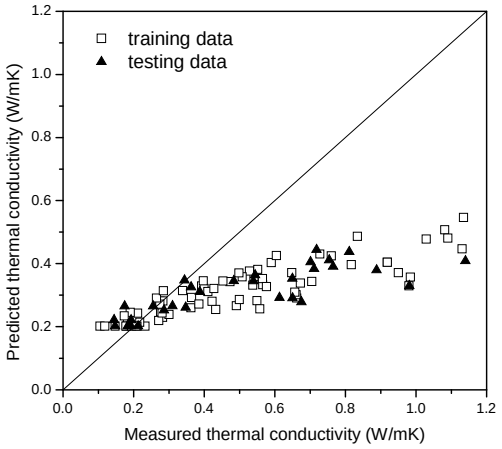

(h) Geometric mean model

Fig. 9 Comparison results of each model

Table 6 Coefficient of determination (R^2) for each estimation model

Method	Coefficient of determination (%)	
	Training data	Testing data
ANNM (Logsig(9)-Tansig)	93	84
3D CSM	72	68
Kersten (1949)	62	59
Johansen (1975)	63	63
Côté and Konrad (2005)	67	66
Lu *et al*. (2007)	65	60
Lee (2010)	14	10
*Geometric mean model	75	68

* Theoretical model

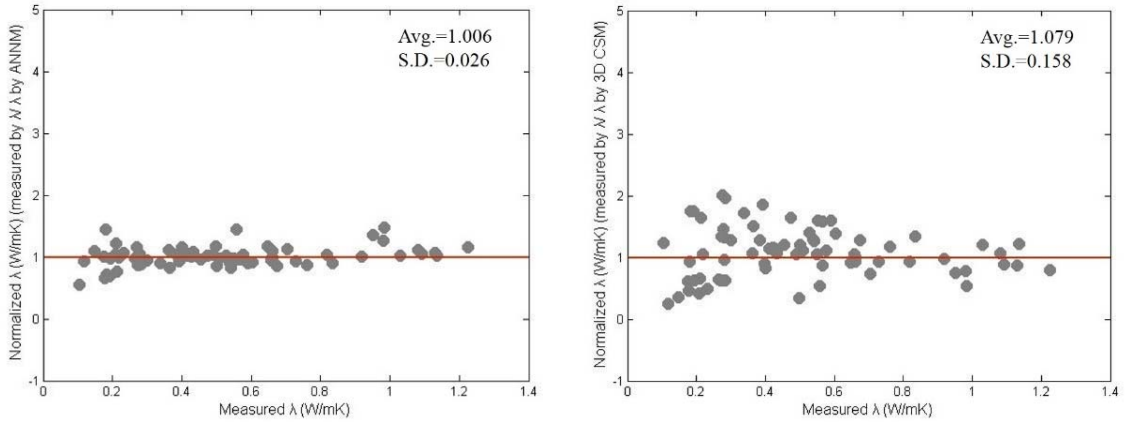

(a) ANNM (b) 3D CSM

Fig. 10 Comparison of normalized thermal conductivity (training data)

conductivity values in considering the distribution pattern. It is because the experimental value itself has a large volatility in low range of thermal conductivity. But it does not have significant physical implication. As for the ANNM, the normalized average values of training and test data were 1.006 and 0.954, respectively, with variations of 0.026 and 0.098. Accordingly, it can be concluded that the ANNM gives much more accurate results than the 3D CSM. Another advantage of the ANNM is that it can improve its accuracy by accumulating more data. Therefore, it has a great potential for the application of it to the estimation of thermal conductivity, for any type of soils in Korea.

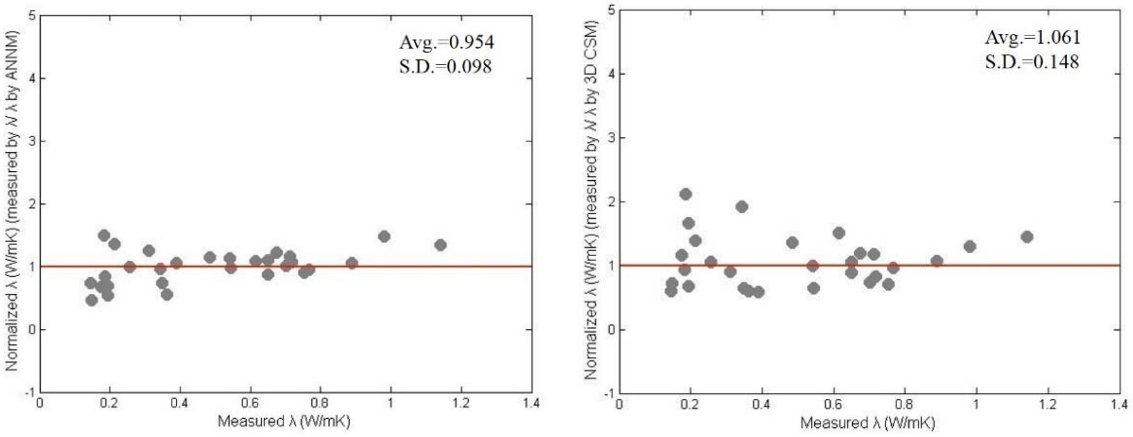

(a) ANNM (b) 3D CSM

Fig. 11 Comparison of normalized thermal conductivity (testing data)

6. Conclusions

This study developed the thermal conductivity database for weathered granite soil in Korea. Based on the experimental data, two empirical models were suggested and verified by comparing the accuracy with others.

The conclusions drawn from this study can be summarized as follows:

- The 3D Curved Surface Model was presented as a function of porosity and moisture content based on the experimental database, and the prediction results showed that the model using only two variables can guarantee adequate accuracy in the prediction of thermal conductivity for weathered granite soils. However, the prediction became unreliable in a low range of thermal conductivity in considering the distribution pattern.
- As for the Artificial Neural Network Model, the 'Logsig-Tansig' transfer function combination gave the highest accuracy estimates.
- The ANNM can consider various input parameters and hence it can provide greater accuracy compared to the previous empirical models.
- The ANNM has also a great potential for the estimation of thermal conductivity for any types of soil in Korea, since it can be improved by accumulating more data.

Acknowledgments

This study was supported by the National Research Foundation of Korea under the Ministry of Education, Science, Technology (under grant No. 2012M3A2A1050974) and the 2011 Construction Technology Innovation Project (11 Technology Innovation E04) by the Korea Institute of Construction and Transportation Technology Evaluation and Planning, funded by the Ministry of Land, Transport, and Maritime Affairs.

References

Bennett, M. (2008), *The Ultimate Ground Source Heat Pump Guide – Part* 4, Geothermal Energy, ZIMBIO, December.

Brandle, H. (2006), "Energy foundations and other thermo-active ground structures", *Geotech*., **56**(2), 81-122.

Côté, J. and Konrad, J.M. (2005), "A generalized thermal conductivity model for soils and construction materials", *Can*. *Geotech*. *J*., **42**(2), 443-458.

Demuth, H. and Beale, M. (1992), User's Guide of Neural Network Toolbox for Use with MATLAB, The Mathworks, Natick, USA.

Farouki, O.T. (1986), *Thermal Properties of Soils*; *Series on Rock and Soil Mechanics*, Volume 11, Trans Tech Publications.

Hart, G.K. and Whiddon, W.I. (1984), "Ground source heat pump planning workshop, Summary of proceedings", EPRI Report RP 2033-12, Palo Alto: Electric Power Research Institute.

Horai, K. (1971), "Thermal conductivity of rock-forming minerals", *J*. *Geophys*. *Res*., **76**(5), 1278-1307.

Hukseflux (2006), User Manual of TP08: Small size non-steady probe for thermal conductivity measurement, Hukseflux Thermal Sensors, Delft, Netherlands.

Johansen, O. (1975), "Thermal conductivity of soils", Ph.D. Thesis, University of Trondheim, Norway.

Kersten, M.S. (1949), Laboratory Research for the Determination of the Thermal Properties of Soils, Research Laboratory Instigations, Engineering Experiment Station, University of Minnesota, Minneapolis,

MI, USA, Tech. Report 23.
Kim, Y.S. (2002), "Feasibility of neural network model application for determination of preconsolidation pressure of soft deposit by piezocone test", *J. KSCE*., **22**(6), 623-633.
Kim, Y.S. (2005), "Development of neural network nodel for estimation of undrained shear strength of Korean soft soil based on UU triaxial test and piezocone test results", *J. KGS*., **21**(8), 73-84.
Laloui, L., Moreni, L. and Vulliet, L. (2003), "Behavior of a dual-purpose pile as foundation and heat exchanger", *Can. Geotech. J*., **40**(2), 388-402.
Lee, G.J. (2010), "Study on thermal characteristics of backfill materials for horizontal ground heat exchanger", Master Thesis, Korea University, Korea.
Lee, Y.G., Yoon, Y.W. and Kang, B.H. (2000), "Prediction of undrained shear strength of normally consolidated clay with varying consolidation pressure ratios using artificial neural networks", *J. KGS*., **16**(1), 75-81.
Lu, S., Ren, T. and Gong, Y. (2007), "An improved model for predicting soil thermal conductivity from water content at room temperature", *SSSA J*., **71**(1), 8-14.
Min, T.K., Hwang, K.M. and Jeon, H.W. (2000), "Prediction of consolidation settlements at vertical drain using modular artificial neural networks", *J. KGS*., **16**(2), 71-77.
Misra, A. and Huang, S. (2011), "Effect of loading induced anisotropy on the shear behavior of rough interfaces", *Tribology Int*., **44**(5), 627-634.
Netzsch (2013), Heat Flow Meters HFM 436 Lambda series, Netzsch, Selb, Germany.
Olgun, C.G., Martin, J.R. and Bowers, G.A. (2012), *Energy Piles*: *Using Deep Foundations as Heat Exchangers*, Geo-Strata, March/April.
Pahud, D., Fromentin, A. and Hubbuch, M. (1999), "Heat exchanger pile system for heating and cooling at Zurich Airport", IEA Heat Pump Centre Newsletter, **17**(1), 15-16.
Park, H.S. (2011), "Thermal conductivities of unsaturated Korean weathered granite soils", Master Thesis, Korea Advanced Institute of Science and Technology, Korea.
Park, H.K., Park, H.S., Lee, S.R. and Go, G.H. (2012), "Estimation of thermal conductivity of weathered granite soils", *J. KSCE*., **32**(2), 69-77.
Penner, E., Johnston, G.H. and Goodrich, L.E. (1975), "Thermal conductivity laboratory studies of some MacKenzie highway soils", *Can. Geotech. J*., **12**(3), 271-288.
Salomone, L.A. and Kovacs, W.D. (1984), "Thermal resistivity of soils", *J. Geotech. Eng*., **110**(3), 375-389.

GC